TEXTE
01/2016

Dynamics of landfast sea ice of Atka Bay, Antarctica

For our Environment

Umwelt Bundesamt

TEXTE 01/2016

Project No. (FKZ) 58740
Report No. (UBA-FB) 002266/ENG

Dynamics of landfast sea ice of Atka Bay, Antarctica

by

Osama Mustafa, Heiko Griebsch, Stefan Knetsch, Christian Pfeifer
ThINK – Thüringer Institut für Nachhaltigkeit und Klimaschutz

On behalf of the German Environment Agency

Imprint

Publisher:
Umweltbundesamt
Wörlitzer Platz 1
06844 Dessau-Roßlau
Tel: +49 340-2103-0
Fax: +49 340-2103-2285
info@umweltbundesamt.de
Internet: www.umweltbundesamt.de

/umweltbundesamt.de
/umweltbundesamt

Study performed by:
ThINK – Thüringer Institut für Nachhaltigkeit und Klimaschutz
Leutragraben 1
07743 Jena

Study completed in:
December 2015

Edited by:
Section II 2.8 Protection of the Arctic and Antarctic
Fritz Hertel

Publication as pdf:
http://www.umweltbundesamt.de/publikationen/dynamics-of-landfast-sea-ice-of-atka-bay-antarctica

ISSN 1862-4804

Dessau-Roßlau, January 2016

The Project underlying this report was supported with funding from the Federal Ministry for the Environment, Nature Conservation, Building and Nuclear safety under project number FKZ 58740. The responsibility for the content of this publication lies with the author(s).

Kurzbeschreibung

Kaiserpinguine (*Aptenodytes forsteri*) brüten in der Antarktis auf dem an der Küste verankerten Meereis (Festeis). Aufgrund des Klimawandels ist das Meereis in vielen Regionen des Kontinents erheblichen Veränderungen ausgesetzt. Um die mögliche Gefährdung einer Kaiserpinguinkolonie in der Atka-Bucht (Ostantarktis) beurteilen zu können, wurden die Veränderungen der lokalen Ausdehnung des Festeises für den Zeitraum 2010/11 - 2014/15 mit Hilfe von Satellitenbildern untersucht. Die Ausdehnung des Festeises wurde für jeden Monat von September bis April im Untersuchungszeitraum räumlich erfasst. Während dieser Zeit bricht das Festeis von Dezember bis Januar auf und erreicht sein Minimum im Februar und März bevor die Bucht im April wieder zufriert.

Bis zur Saison 2010/11 konnte weder eine signifikante Abnahme noch ein Anstieg der Eisbedeckung anhand der verfügbaren Daten festgestellt werden. Danach wurde ein deutlicher Anstieg der Eisbedeckung verzeichnet. Ob es sich hierbei um ein klimatologisches Signal oder um die Auswirkungen eines singulären Ereignisses, dem Stranden eines großen Eisberges, welcher den nördlichen Teil der Akta-Bucht von August 2012 bis Juli 2013 blockierte, handelt, müssen die Beobachtungen kommender Saisons zeigen.

Die Analyse des räumlich-zeitlichen Musters offenbarte die Existenz einer robusteren Zone im Südwesten der Atka-Bucht. Das Festeis bricht hier später in der Saison auf und friert bereits früher wieder zu.

Durch die räumliche Erfassung der Flächen die von den Pinguinen seit 1984 als Brutgebiete genutzt wurden, stellte sich heraus, dass die Kolonie überwiegend die robustere Zone nutzt, selbst wenn die gesamte Bucht eisbedeckt ist.

Soweit die verfügbaren Daten eine Aussage erlauben, wurde kein Anzeichen dafür gefunden, dass die Kaiserpinguinkolonie in der Atka-Bucht durch eine veränderte Dynamik des Festeises kurzfristig bedroht wird.

Abstract

Emperor penguins (Aptenodytes forsteri) breed on Antarctic landfast sea ice in regions dramatically impacted by climate change. To assess endangerment of an emperor penguin colony in Atka Bay (East Antarctica), local extent changes of landfast sea ice have been studied for the period 2000/01 - 2014/15 aided by satellite images.

Landfast sea-ice extent was measured for each month from September to April in the above study period. In Antarctica, ice breaks up from December to January, reaching its minimum in February and March; the bay freezes again in April. No significant year-to-year ice-coverage trend was recorded by the available data until season 2010/11. Later a distinct increase of ice coverage was recorded. Observations of future seasons will show whether this increase is an indication of changing climatological conditions or a singularity caused by a large grounded iceberg that blocked the northern part of the bay from August 2012 to July 2013.

Analysis of the spatio-temporal pattern revealed the existence of a robust ice zone in the southwestern part of Atka Bay. In robust zone, landfast sea ice breaks up later in the season and forms earlier.

By delineating the area used by the penguins as breeding site since 1984 it was found that the colony predominantly uses the robust zone even if the whole bay is frozen.

Available database evidence does not support short-term threat to emperor penguin colony of Atka Bay due to changing dynamics of landfast sea ice.

Table of contents

List of figures

List of tables

List of abbreviations

AABW	Antarctic Bottom Water
ALOS	Advanced Land Observing Satellite
ERS	European remote sensing satellite
GIS	Geographic Information System
MODIS	Moderate Resolution Imaging Spectroradiometer
PALAOA	Perennial Acoustic Observatory in the Antarctic Ocean
PALSAR	Phased Array type L-band Synthetic Aperture Radar
PAN	panchromatic band
RGB	color model representing visible light spectrum by combining red, green and blue
SAR	synthetic aperture radar
SWIR	shortwave infrared
VNIR	visual & near-infrared spectral range

1 Introduction

Emperor penguins (*Aptenodytes forsteri*) breed on Antarctic landfast sea ice, which is dramatically impacted by climate change in many regions of the continent. Within the context of Antarctic sea ice, the study analyses the dynamics of landfast sea ice in Atka Bay of east Antarctic. Finally, the study assesses impact of possible sea-ice changes on the emperor penguin colony breeding in the area.

1.1 The Antarctic sea ice

Sea-ice cover in the Antarctic is trending positively (increasing), in contrast to the Arctic, as demonstrated in passive microwave data obtained since late 1970s (Zwally 2002; Parkinson and Cavalieri 2012; Schneider et al. 2012). This increasing trend applies both to sea-ice extent and to sea-ice area, two parameters that describe quantity of sea ice. Although increase of sea-ice area can be seen as more significant than the increase of extent (Liu 2004). The extent refers to the summed area in a certain region with a sea-ice concentration of at least 15% whereas sea-ice area refers to the actual amount of ice, which is explained by the product of sea-ice extent and sea-ice concentration. (Parkinson and Cavalieri 2012).

Ice coverage trends differ from region to region. The increasing trend of sea ice cannot be noted for the whole Antarctic continent, however, and the Antarctic Peninsula presents a particular exception. Here, both a decrease of sea-ice extent and area can be observed, in a local regional context that is also experiencing increasing temperature. Not only the Peninsula shows the trend of a decreasing sea-ice extent and area; similar results are obtained in the Bellingshausen and Amundsen Sea. In each month of the studied season (September to April) the same negative ice (not temperature) trend can be observed (Parkinson and Cavalieri 2012). Nevertheless, the negative ice trends of these regions can be considered exceptions in the Antarctic context as a whole. West and east Antarctic regions present generally opposing trends: The western part (including the peninsula) presents a warming trend combined with a decrease of sea ice. In the east, nine out of thirteen stations show a cooling trend over the years that can be linked to the increasing sea-ice extent and area (Vaughan et al. 2003). The Ross Sea is an example where not only an increase of sea-ice extent and concentration is recorded, but also ice-season duration (Schneider et al. 2012).

The Weddell Sea also shows a positive trend. Except for the northwestern part, an increase of sea-ice concentration could be observed from 1979-2013 (Turner et al. 2015a). Along the eastern coast ice increase is about 2.5% per decade (Teschke et al. 2015; Schwegmann 2012). Particularly during the summer months a large increase can be noticed with an increasing trend of sea-ice concentration of 15% or more per decade (Teschke et al. 2015).

Observations show that the minimum value of Antarctic ice extent in February has decreased over the last years whereas the maximum value in September has increased (Comiso & Nishio 2008). Since 1979 the annual maximum extent of sea-ice „has increased by 1% per decade“ (Reid et al. 2015, p. 99). The largest trend of sea ice increase around the continent can be observed in autumn (March – May) and the smallest in summer (December – February). The largest increases have been measured in the years 2003, 2008 and 2013 (Turner et al. 2015). An absolute maximum of sea-ice extent was recorded on 30th of September 2013 as a result of a steady above-average growth of sea-ice extent and area during the whole year (Reid et al. 2015).

These observed trends in sea-ice evolution do not reflect global climate models. Global-model simulations predict a loss of sea ice in the 21st century, with reductions between 10% and 50% of sea-ice concentration in winter and between 33% and a total loss of sea ice in summer (Sen Gupta et al. 2009). Present global models are characterized, above all, by significant uncertainty (Arzel et al. 2006). Turner et al. (2013) state that climate models generally fail to correctly predict Antarctic sea-ice evolution. Climate-model simulations show a decrease of sea-ice extent and area, demonstrating the incompleteness of the models. Another remarkable point is that results obtained by different models do not coincide with each other. Simulated responses of sea ice to a CO2-increase show a large range and "it appears that the warming response and the sea-ice response are not uniformly related in the current generation of climate models, and the range in this relationship amongst models reflects an underlying lack of ability to correctly model the complex inter-related feedbacks within the climate system, some of which involve sea ice" (Flato 2004, p. 240). This leads to the assumption that those models lack of some key processes that influence the sea-ice evolution (Hoppmann et al. 2015b). Bintanja et al. (2013) for example consider the accelerated basal melting of the ice shelves as a key factor, leading to the increasing sea ice.

As different models failed to correctly predict the sea ice evolution in the past and present, it cannot be expected that they will provide reliable future projections.

1.2 Antarctic landfast sea ice

Landfast sea ice is a subclass of fast ice. Fast ice is defined as "sea ice which forms and remains fast along the coast, where it is attached to the shore, to an ice wall, to an ice front, between shoals or grounded icebergs" (WMO 2014, p. 6). Landfast sea ice is fast ice that is held stationary (fast) by being attached to coastal features (e.g., the shoreline, glacier tongues, and ice shelves) (Fraser et al. 2012).

Antarctic landfast sea ice is significant for both climatic and ecological reasons: First, and important for the focus of this study, it plays a crucial role in the life cycle of emperor penguins and Weddell seals (Massom et al. 2009). Furthermore, landfast sea ice is closely associated with coastal polynyas, which have far-reaching consequences in terms formation of Antarctic Bottom Water (AABW) and hence the global thermohaline circulation (Fraser et al. 2012).

In comparison to sea ice as a whole, relatively little is known about larger-scale aspects of Antarctic fast-ice distribution and variability in space end time (Fraser et al. 2012). Nihashi & Ohshima (2015) investigated the connection between landfast sea ice and polynya and showed that the change in fast-ice extent, which is particularly vulnerable to climate change, causes dramatic changes in the polynyas and possibly AABW formation that can potentially contribute to further amplification of climate change. Kim et al. (2015) found that the residence time of fast ice was much shorter in the West Antarctic than in the east. Fraser et al. (2012) investigated the quantitative extent of landfast sea ice in East-Antarctica between 2000 and 2008 and found a statistically significant in-crease of 1.43 % per year. Regionally, there is a strong increase in the Indian Ocean sector of East-Antarctica (20°E to 90°E) of 4 % per year.

An important driver for ice dynamics in the Antarctic is the forming of platelet ice. It forms and grows in super-cooled water, which originates from ice shelf cavities Platelet ice is a direct indicator of ocean/ice-shelf interaction, and the amount of basal ice-shelf melt might be reflected by the volume of ice platelets found below landfast sea ice (Langhorne et al. 2015).

The high variability of ice platelets strongly influences the spatial and temporal variability of fast-ice mass balance in Atka Bay. Hoppmann et al. (2015b) found at this location an average platelet-layer thickness of 4m by December 2012, with local maxima of up to 10 m and an average ice-volume fraction in the platelet layer of 25%.

1.3 Landfast sea ice and emperor penguins

It is difficult to estimate the total number of emperor penguins living in the Antarctic. Distances of concerned breeding habitats to research stations hamper access. Existing satellite images are often not clear enough to distinguish between penguins, shadows and guano (Fretwell et al. 2012). Also, questions remain whether all colonies have been detected (Fretwell and Trathan 2009, Ancel et al. 2014). Fretwell et al. (2012) assume a total number of emperor penguin colonies of 46. In 2009, they estimated the number of individuals of every colony, resulting in the aggregate estimate of 595,000 adult emperor penguins (Fretwell et al. 2009). By 2014, 52 colonies were identified (Fretwell & Trathan quoted by Ancel et al. 2014).

Figure 1: Schematic representation of key dates in the emperor penguin annual breeding cycle at Pointe Géologie, Adélie Land

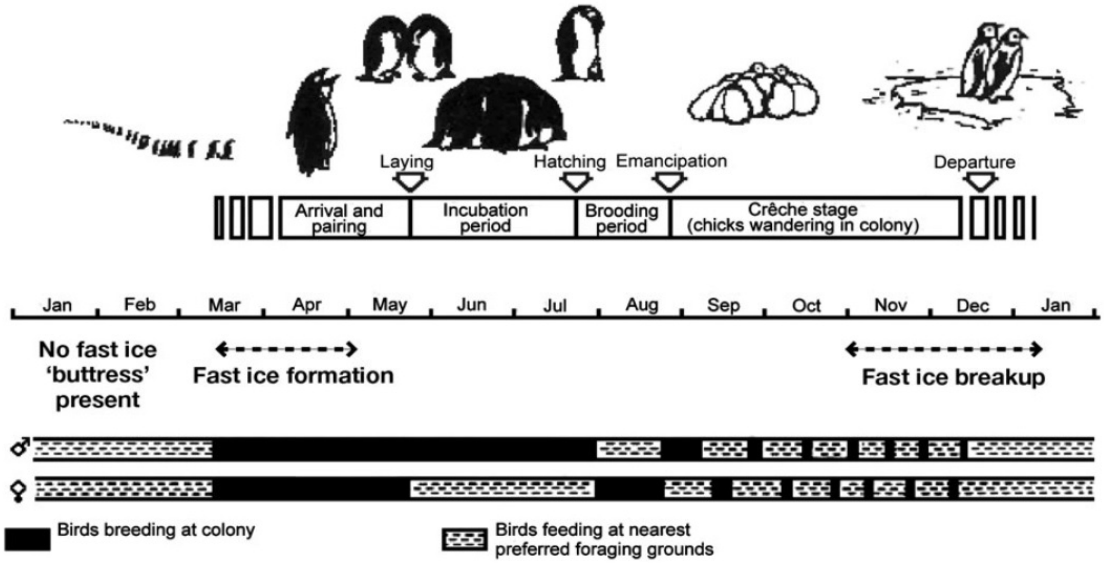

Massom et al. 2009 (after Jouventin et al. 1995)

Breeding sites can be located throughout the whole coastline of the Antarctic continent (Fretwell et al. 2012). Breeding and raising offspring, foraging and moulting take place on landfast sea ice (Jenouvrier et al. 2009; Jenouvrier et al. 2014). Emperor penguins' life cycle depends strongly on the characteristics of the sea ice and investigations on the breeding behavior of a colony in Adélie Land (Jouventin et al. 1995; Massom et al. 2009, see Figure 1) show that emperor penguins get together in breeding colonies after the formation of fast ice in March/April. After laying eggs in mid-May, male penguins remain in order to incubate the eggs, while the females leave for feeding and come back to supersede the males in late July when the eggs hatch. Males and females alternate parental roles as the chicken grows and its crêche stage begins after about 50 days during which they are fed by both parents. In December/January the penguins finally depart the colony with surviving chicks. Breeding patterns in Adélie Land apply in principle to other emperor penguin colonies of the Antarctic as well, with minor local variations.

Since breeding takes place completely on landfast sea ice, emperor penguin populations are sensitive to sea-ice changes potentially resulting from climate change. More dense and extensive sea ice is detrimental for penguin breeding because of longer foraging trips. Predicted sea-ice decline is also detrimental because of breeding habitat loss. Sea-ice conditions projected by coupled climate models would indicate a dramatic decrease of emperor penguin population. Global population estimates for

2100 are 19% lower compared to 2009, with a temporary peak in 2048. Threat is very diverse for different colonies. The colony of Atka Bay is assessed to a conservation status of "Quasi-extinct" in 2100. (Jenouvrier et al. 2014)

In this case "emperor penguins will have to adapt, migrate or change the timing of their growth stages" to avoid foreseeable extinction like Jenouvrier et al. (2009, p. 1844) stated for a colony in Terre Adélie. Since 2009 a few breeding colonies have already been observed on ice shelves instead of sea ice during breeding season. One of them was the colony at Atka Bay, even though the sea ice there has been stable (Fretwell et al. 2014; Zitterbart et al. 2014).

2 Methods and Data

2.1 Study area

Located at the eastern part of the Weddell Sea, the Atka Bay (70°36'S, 8°08'W) has an extent of about 20 x 30 kilometers. The annual averaged temperature is -16.1°C at Neumayer Station, the German wintering research station, situated about 6 km to the west of Atka Bay. The coldest month is July with a mean temperature value of around -23°C, a minimum value of around -45°C and -3°C being the maximum temperature. December and January are usually the warmest months with a mean temperature of around -3°C, and a range from -20°C to +5°C in December (from -23°C to 3°C in January) (König-Langlo and Loose 2007). The dominant winds are easterlies. Storms with wind speeds above 30 m per second are common; the average is 9 m per second (König-Lango and Loose 2007). The mean wind speed increases from January (7 m per second) until August, reaching a peak of 11 m per second. This shows clearly that the winter with its monthly mean wind speed close to/above 10 m tends to be much windier than the summer (van den Broeke et al. 2010). In 2012, the windiest day was August 6, with a speed of 34 m per second measured. In the same year the most windless months were April and July (Hoppmann et al. 2015b). The direction of weaker winds usually has a southerly wind component (Klöwer et al. 2013). Precipitation, usually snow, can be expected in all months. The mean annual accumulation rate is about 340 mm water equivalent. During summer, drizzle and rain are also possible. On average, the sun shines 1430 hours annually (König-Langlo and Loose 2007).

The Atka Bay is mostly covered with fast ice that forms between March and April, growing until December, and then reaching its maximum thickness. The break-up of the sea ice usually takes place between December and January as a consequence of factors like changes in water and air temperature and wind conditions. The fast ice of Atka Bay is of importance for emperor penguins as it is the breeding ground for one large colony (Hoppmann et al. 2013; König-Langlo et al. 1998). Measurements from 2013 indicate that the temperature of the sea water was "below the surface freezing point between April and November 2013, with a minimum in late May" (Hoppmann et al. 2015b, p. 1715). The freezing point most of the time was at -1.87°C increasing to -1.85°C in May when the salinity was lowest. The sea water temperature was measured at a depth of 155 m at PALAOA (Perennial Acoustic Observatory in the Antarctic Ocean) at Atka Bay and varied between -1.75°C and -1.85°C (7 day running mean) from December-February and between -1.85°C and -1.95°C from March-November (Hoppmann et al. 2015b). Particularly, because of the measuring depth it is only of limited transferability to the near surface conditions at Atka Bay. However, more data have not been available.

This study defined the concrete area of investigation as a rectangle 30 x 20 kilometers (Figure 2). If reduced by the shelf ice covered area, the study site has a total of 470 square kilometers.

Figure 2: Atka Bay and study area

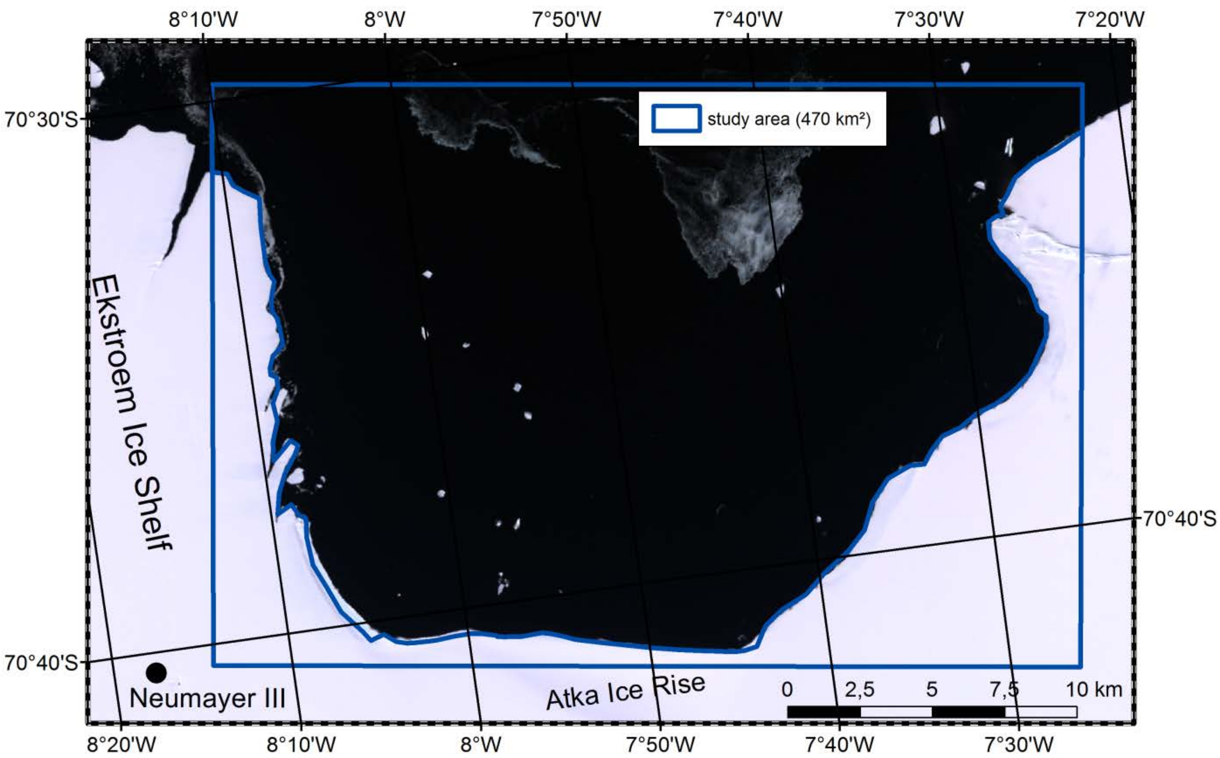

Background image Landsat 7 (15 Jan 2011); by courtesy of NASA GSFC & USGS

2.2 Satellite imagery

2.2.1 Landsat

Landsat satellites have continuously acquired remote sensing data of the earth's surface from 1972 until present time. Eight Landsat satellites (Landsat 6 didn't reach orbit) were sent to space over this period and two are still operational (Figure 3). Each satellite is equipped with a sensor possessing different spatial and spectral characteristics (Table 1). The first satellites only had a ground resolution of 60 m (actually 79 x 57 m pixels but resampled to 60 m) and only 4 spectral bands (3 bands in visible spectrum and 1 in near-infrared). Later satellites increased the ground resolution (30 m) and the spectral resolution with up to 8 spectral bands (4 bands in visible spectrum, 1 near-infrared band and 3 SWIR bands for Landsat 8). This high spectral resolution allows a fast and easy discrimination of ice and clouds in the image with the band combination of blue - SWIR 1- SWIR 2 (Landsat 7 = 357, Landsat 8 = 467; USGS 2015).

Figure 3: Landsat mission characteristics

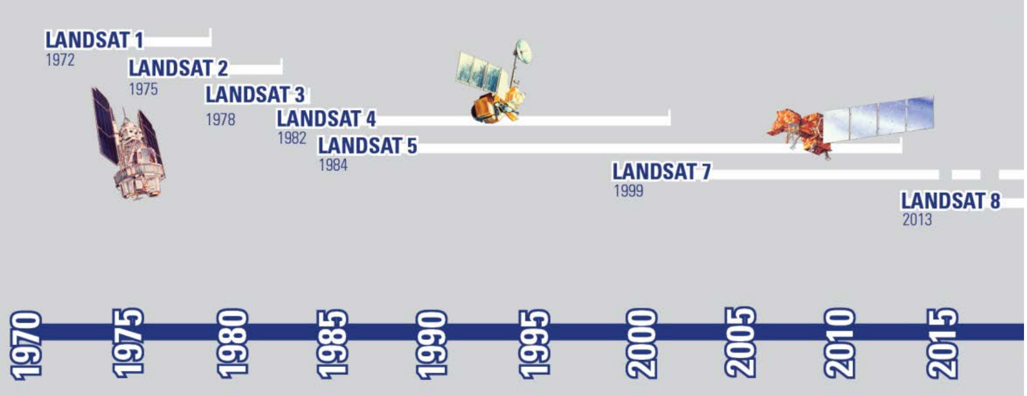

(USGS 2015)

Table 1: Landsat satellites basic sensor characteristics

Satellite	Sensors used in this study	Ground resolution of multispectral bands [m]*	Spectral resolution*
Landsat 1-5	MSS	60	4 bands (VNIR)
Landsat 4-5	TM	30	4 bands (VNIR)
Landsat 7	TM+	30	6 bands (VNIR+SWIR)
Landsat 8	OLI	30	8 bands (VNIR+SWIR)

*without thermal and PAN band

2.2.2 Terra – MODIS

Both, Terra (launched December 1999) and Aqua (launched May 2002) satellite are equipped with the MODIS sensor (Moderate Resolution Imaging Spectroradiometer). They have a very high repetition rate of 1 or two 2 days. Of the total 36 available spectral bands this study utilized only 7 which are combined in the “Surface Reflectance product” offering the highest ground resolution available at Atka Bay. From 2000 until 2012 only the product “MOD09GA” is available with a ground resolution of 500 m. For the period since Mai 2012 it was possible to get datasets with 250 m ground resolution (MOD09GQ). Both Surface Reflectance products provide 7 spectral VNIR-SWIR bands comparable of those of Landsat. In this study only MODIS data from Terra were used as its image archive reaches 2 years more in the past by reason of its earlier start (Vermote et al. 2011).

2.2.3 ALOS – PALSAR

Radar data from the Advanced Land Observing Satellite (ALOS) acquired with the PALSAR (Phased Array type L-band Synthetic Aperture Radar) instrument were used in the study if appropriate images were available. The satellite was launched in January 2006 and stopped working May 2011. Both the Fine-Mode data with 12.5 m and the ScanSAR-Mode data with 100 m ground resolution were used. The main advantage of the PALSAR instrument is its independence from weather or sunlight conditions because the Microwave L-Band (1270 MHz) used by the sensor is able to interpenetrate even heavy cloud cover (Japan Aerospace Exploration Agency 2015).

2.2.4 ERS – SAR

ERS-1 and ERS-2 are almost identically constructed European remote sensing satellites. ERS-1 has been operating from 1991-2000 and ERS-2 from 1995-2005. At both satellites a synthetic aperture radar (SAR) collected data at the C-band (5.6 cm) allowing data acquisition independent from cloud-cover and sunlight. In the study only a few georeferenced quicklooks of ERS-2 images had been used (Attema et al. 2000).

2.3 Available data

To assess the dynamics of landfast sea ice at Atka Bay, different satellite platforms were used. If available, Landsat imagery was the primary data source. In many cases a dense cloud cover prevented the use of an image, occasionally the Scan Line Corrector failure (NASA, National Aeronautics and Space Administration 2011) did likewise for some of the Landsat 7 ETM+ images. The chosen temporal resolution is one dataset per month. The period May to August were excluded from the analysis as almost no imagery was available during the polar night and the coverage of the study area by fast ice could be assumed as 100 %. If more than one analyzable image was available, that one was selected which is the closest to the 15th of the month. Synthetic Aperture Radar (SAR) imagery from ALOS-PALSAR system was used as secondary data source, with the advantage of being able to interpenetrate even heavy cloud cover. The third data source was the MODIS sensor on board of the Terra (EOS AM-1) satellite. Due to its high repetition rate and its high spectral resolution, which allowed a good distinction of clouds and ice, these data helped to fill the gaps. Therefore it was possible to get information for every month from season 2000/01 to 2014/15. For the years before MODIS data were available, a proposal was submitted to the European Space Agency (ESA) to get access to SAR data of the ERS-1/2 missions. The proposal was not answered until the completion of this report. As without these data the gaps were to large, the analyses were only done for the mentioned period (Table 2).

Table 2: Satellites which data was available for this study

	Sep.	Oct.	Nov.	Dec.	Jan.	Feb.	Mar.	Apr.
2014/15	L8*	L8	Terra	L8	Terra	Terra	Terra	Terra
2013/14	Terra	Terra	L8	L8	L8	L8	Terra	Terra
2012/13	Terra	Terra	L7	L7	L7	L7	L7	Terra
2011/12	Terra	Terra	L7	L7	L7	L7	L7	Terra
2010/11	Terra	Terra	L7	L7	L7	Terra	L7	Terra
2009/10	Terra	Terra	L7	L7	L7	L7	L7	Terra
2008/09	ALOS	Terra	L7	L7	L7	L7	Terra	Terra
2007/08	ALOS	ALOS	ALOS	L7	L7	L7	L7	Terra
2006/07	Terra	Terra	Terra	L7	Terra	L7	L7	Terra
2005/06	Terra	Terra	Terra	Terra	Terra	Terra	Terra	Terra
2004/05	Terra	Terra	Terra	Terra	Terra	Terra	Terra	Terra
2003/04	Terra	Terra	Terra	Terra	Terra	Terra	Terra	Terra
2002/03	Terra	Terra	L7	L7	L7	Terra	Terra	Terra
2001/02	Terra	Terra	Terra	L7	Terra	Terra	Terra	Terra
2000/01	Terra	Terra	L7	L7	Terra	Terra	Terra	Terra

1999/00				L7	L7	L7	Terra
1996/97					L5	L5	
1995/96	ERS						ERS
1994/95					ERS		
1989/90		L4	L4	L4			
1987/88	L5	L4		L4	L4	L4	
1985/86				L5	L5	L5	
1984/85			L5	L5	L5	L5	
1975/76		L2					
1974/75					L2		
1973/74			L1	L1			

*L = Landsat

2.4 Delineating of landfast sea ice

The delineating of landfast sea ice was done by help of a Geographic Information System (GIS). The outlines of the ice where captured from the satellite images. In this study, only the landfast sea ice (fast ice that is attached to the shore, in this case the ice shelf) was considered (see chapter 1.2). Fast ice that is frozen to icebergs or mobile sea ice is not the objective of this study and was therefore not delineated. The area of landfast sea-ice extent was calculated by using the GIS and for calculating the relative area the coastline of the bay and the outline of the study area (see Figure 2) were used as reference.

To make the difference between ice and open water as clearly visible as possible a certain band combination was applied for Terra and Landsat images. This band combination used the bands Blue - SWIR 1- SWIR 2 to allow a clear discrimination of clouds (white color) and ice (red color) which otherwise look very similar (both white) at the standard RGB band combination. This was required since in many images clouds were present near or over the study area.

Main reason for preferring manual delineation to automatic or semi-automatic classification methods was the more precise an efficient identification of polynyas. Their reflection signature in many cases is very close to that of sea ice. Therefore structural and textural differences had to be used to distinguish both features. This particularly is the case for Terra images due to coarse spatial resolution.

2.5 Emperor penguin colony

The population size of the emperor penguin colony of Atka Bay was for the first time examined by Hempel & Stonehouse (1987) which stated a number of 8000 chicks in Oct/Nov 1986. Van Franeker et al. (2010) counted 11,000 chicks and 1,200 adults on 14 December 2007. Latest numbers were presented by Fretwell et al. (2012) with a population estimate of 9657 breeding pairs for 2009. .

To examine the impact of the seasonal fast-ice alterations at Atka Bay, the location of the colony was derived from the same satellite images as used for the fast-ice detection. Because of the relative small size of the penguin colony it was only visible in the Landsat images. According to the approach of Pfeifer et al. (2013) the guano covered areas have been manual delineated.

The focus of this study was not on the absolute size of the colony but on the distribution of the area where penguins have been present during the breeding period. Thus, not only the current position of the penguins was included but also older guano stains that indicated a longer stay of penguins at the area. This implies, that the delineated area not only represents the position of the colony at the moment of image recording but, depending on the weather conditions (snow, wind) possibly also the positions of days or weeks before.

Figure 4: Detail of the emperor penguin colony at the Atka Bay (WorldView-2 bands 832) (3 Sept 2012)

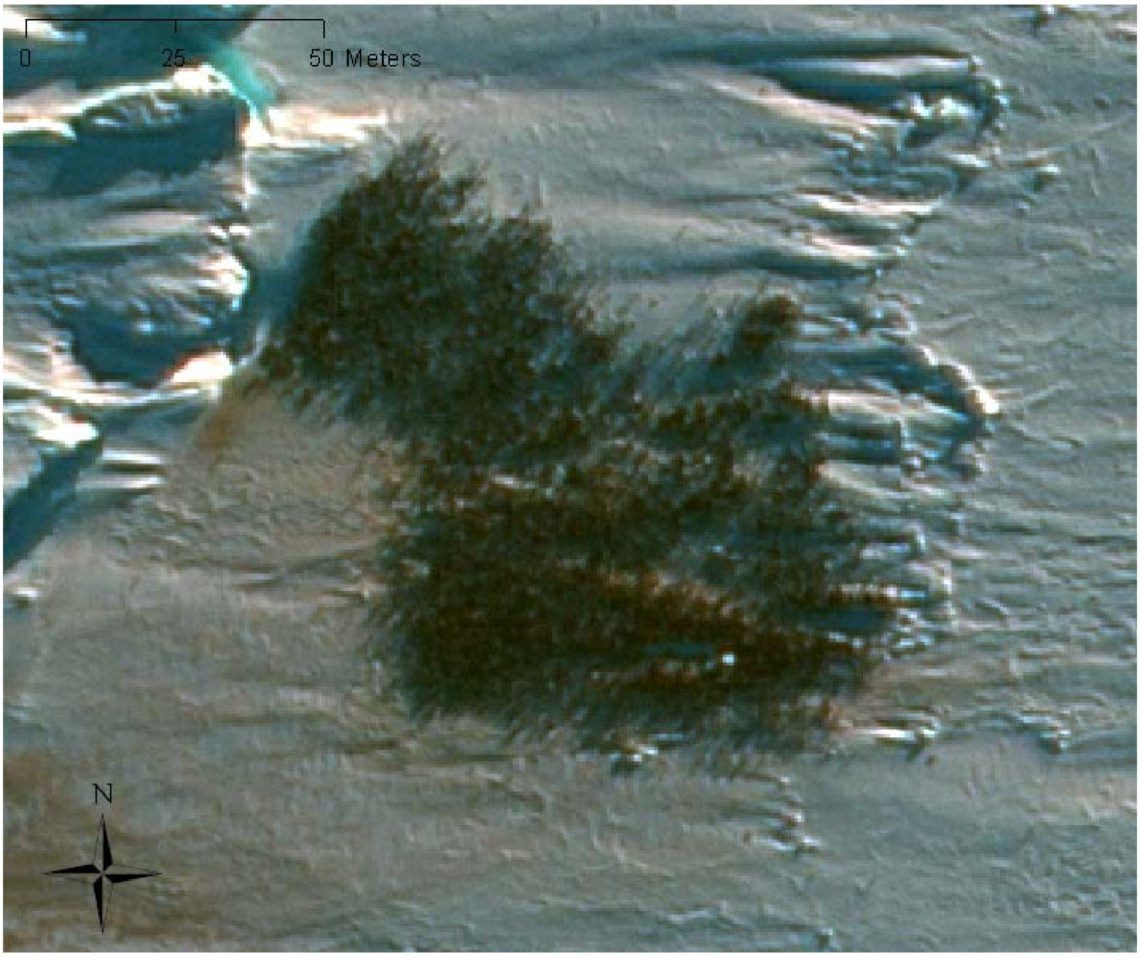

WorldView-2, 50 cm ground resolution, © Digitalglobe 2012

3 Results

3.1 Total ice coverage

The extent of the landfast sea-ice cover in Atka Bay depends on the strength of winds and ocean currents offshore and as well on the interaction with frequently passing icebergs (Hoppmann et al. 2015). Besides this, seasonal changes are significant. The observation window of this study ranges from the austral spring (September) to the beginning of austral autumn (April). Figure 5 shows the landfast sea-ice cover of Atka Bay in percent of the total area. In September, the mean value of the landfast sea-ice cover in the study area is 84%. The ice cover still grows until October and reaches its maximum in this month (91.7%). Satellite images show, that a coastal polynya is frequently developed in that time that separates the landfast sea ice from the mobile sea ice north of Atka Bay. Starting in November, the mean fast-ice cover is slowly decreasing during November and December. In January, the break-up of the fast ice is accelerating and reaches minimum mean values in February and March (16%).

Figure 5: Total landfast sea-ice cover of Atka Bay in percent

	Sep	Oct	Nov	Dec	Jan	Feb	Mar	Apr
2014/15	96,8	97,7	99,2	88,1	88,3	82,0	92,3	92,6
2013/14	100,0	100,0	97,6	94,7	94,4	33,2	56,9	96,8
2012/13	71,8	100,0	100,0	99,2	97,1	86,1	85,4	82,1
2011/12	70,9	100,0	100,0	100,0	81,3	89,3	0,0	62,4
2010/11	94,6	91,9	89,6	28,0	0,0	8,2	13,2	72,4
2009/10	97,9	89,4	98,5	98,0	86,7	0,0	15,0	53,7
2008/09	100,0	100,0	99,9	99,9	0,0	3,6	0,0	9,2
2007/08	100,0	97,1	89,3	92,2	90,7	8,9	0,0	24,5
2006/07	56,1	94,7	98,1	70,4	72,1	0,0	0,0	54,5
2005/06	75,2	79,3	78,1	55,7	39,6	0,0	0,0	22,9
2004/05	68,5	73,6	66,0	62,1	53,2	0,0	22,4	30,2
2003/04	85,6	85,3	75,7	71,4	69,4	17,3	4,5	20,5
2002/03	88,5	91,0	90,9	79,7	78,5	0,0	0,0	53,4
2001/02	72,7	70,0	75,3	84,6	78,4	0,0	0,0	50,7
2000/01	85,7	97,3	95,1	80,6	76,6	17,7	7,1	80,1
1999/00					98,5	3,7	0,0	57,8
1998/99								
1997/98								
1996/97						0,0	19,7	
1995/96		0,0						91,0
1994/95						0,0		
1993/94								
1992/93								
1991/92								
1990/91								
1989/90			87,9	82,3	22,8			
1988/89								
1987/88		100,0	100,0		72,4	0,0	0,0	
1986/87								
1985/86					0,0	0,0	12,4	
1984/85				79,7	66,8	0,0	0,0	
1983/84								
1982/83								
1981/82								
1980/81								
1979/80								
1978/79								
1977/78								
1976/77								
1975/76			50,4					
1974/75						0,0		
1973/74				94,9	28,2			
1972/73								

at least partial covered by landfast sea ice

no landfast sea ice

no data

Figure 6 shows the distribution of the data for each month. The first month of a season considered in this study is September and shows a medium statistical diversion. The median (394 km²) is still lower than for the next month, because the ice cover is still growing in this month of early austral spring. Furthermore, as seen in the satellite images, there is often a coastal polynya in the northern part of the bay, which is formed by katabatic winds blowing from the ice shelf (Heinemann et al. 2013).

The statistical diversion of the landfast sea-ice cover is lowest in October and November. Here, in the austral spring, the highest ice coverage is observed (median of about 415 km²). Short whiskers in Figure 6 indicate a low statistical dispersion. There is just one "mild" outlier in October 2001 with 321 km² ice cover. In December and January, at the beginning of the austral summer, the median values of ice coverage in Atka Bay decrease (368 and 308 km² respectively) while the dispersion of values increases. In December 2011, the bay was still completely covered with fast ice, and in December 2010 it has been already broken-up until 72 % of the area was ice free. In January, the variability of fast-ice cover is even higher than in December. The values are ranging from 445 km² in January 2013 to completely ice free conditions in 2009 and 2011. In February (median 37 km²) and March (median 30 km²), the landfast sea-ice cover of Atka Bay reaches its lowest values. In February, in 6 of 15 considered years, no landfast sea ice was in the bay. But there are three "mild" outliers in February, regarding the years 2012, 2013 and 2015, where landfast sea-ice cover still had an area of up to 410 km².

In April, the refreezing of the ice cover is starting and the highest statistical diversion of the ice covered area can be found in this month. The median ice cover in April is 247 km², with a minimum value of 42 km² in 2009 and maximum value of 444 km² in 2014. Obviously, the timing of refreezing is very different.

Figure 6: The seasonal development of landfast sea-ice cover at Atka Bay

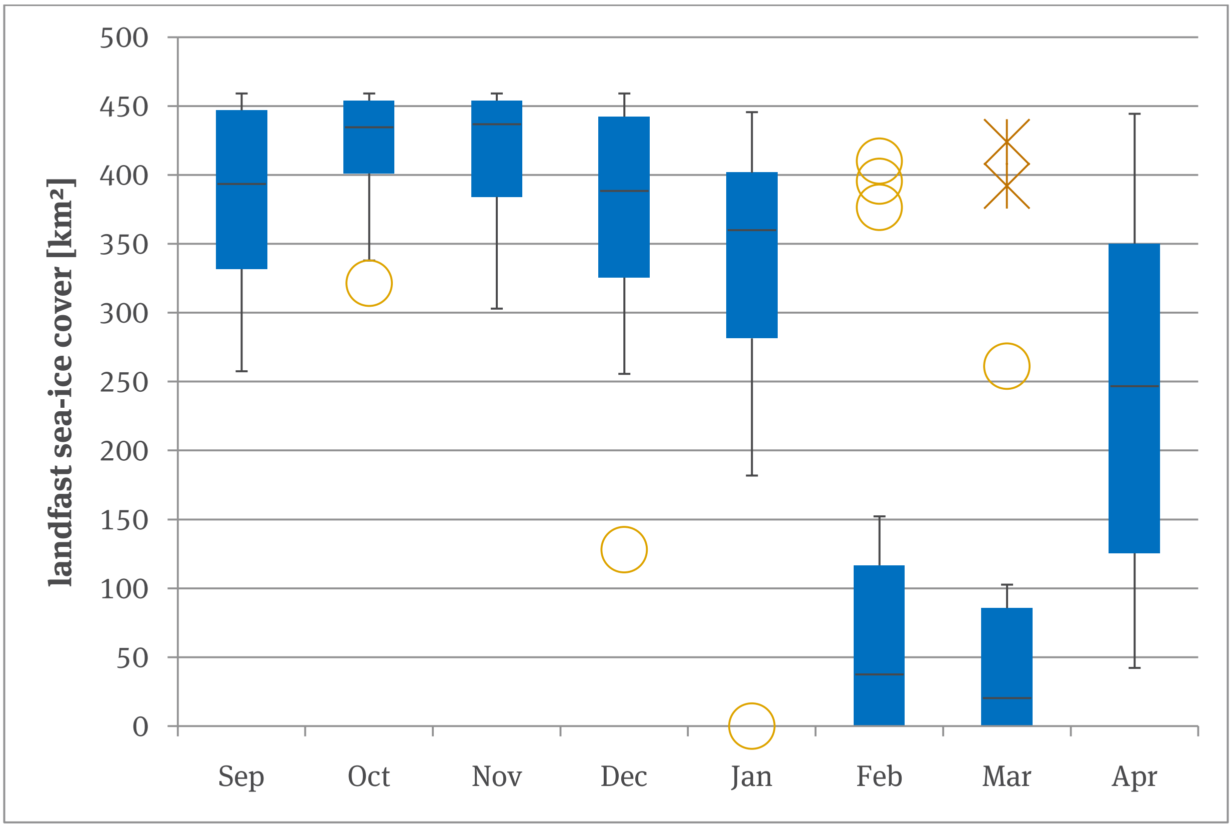

As shown in Figure 7, the temporal evolution of the fast-ice cover of Atka Bay can be separated into two sections. Firstly, from 2000/01 to 2010/11 there is no significant trend in the mean landfast sea-ice cover of the considered months. A local minimum of the seasonal mean values occurs in the seasons 2003/04 to 2005/06, where the lowest values of mean ice coverage are found. This is particularly clear in November, December and January, where the ice coverage is distinctly lower as in the other years (Figure 8). Beginning from 2011/12, there is a distinct increase of the mean values of the landfast sea-ice cover. This trend is particularly noticeable in February and March (see Figure 8). Here, from 2000 to 2011, only in five years a minor fast-ice cover (less than 20 %) remains in the Bay. From 2012 to 2015 (in March from 2013 to 2015) there is always a certain amount of fast ice in Atka Bay, which survived the last summer and became second year ice. From August 2012 to July 2013, a large grounded iceberg (B15G, about 15 km diameter) blocked the northern part of Atka Bay. As a consequence, ice dynamics in the study area was at least partly controlled by this blocking situation. The fast ice survived the summer and became thick second-year sea ice in 2013. The minimum ice cover in season 2013/14 was 152 km² (33 %) in February 2014. In the next season the minimum ice cover occurred again in February, but with much higher values (376 km²/ 82 %). Because of the short period of distinct higher fast-ice coverage and the lack of suitable meteorological and oceanographic data it can only be speculated, whether the reason for the larger ice cover is the thicker multi-year landfast sea ice, as a result of the blocking situation or of changing climatological or oceanographic conditions.

Figure 7: Temporal evolution of the mean landfast sea-ice cover at Atka Bay

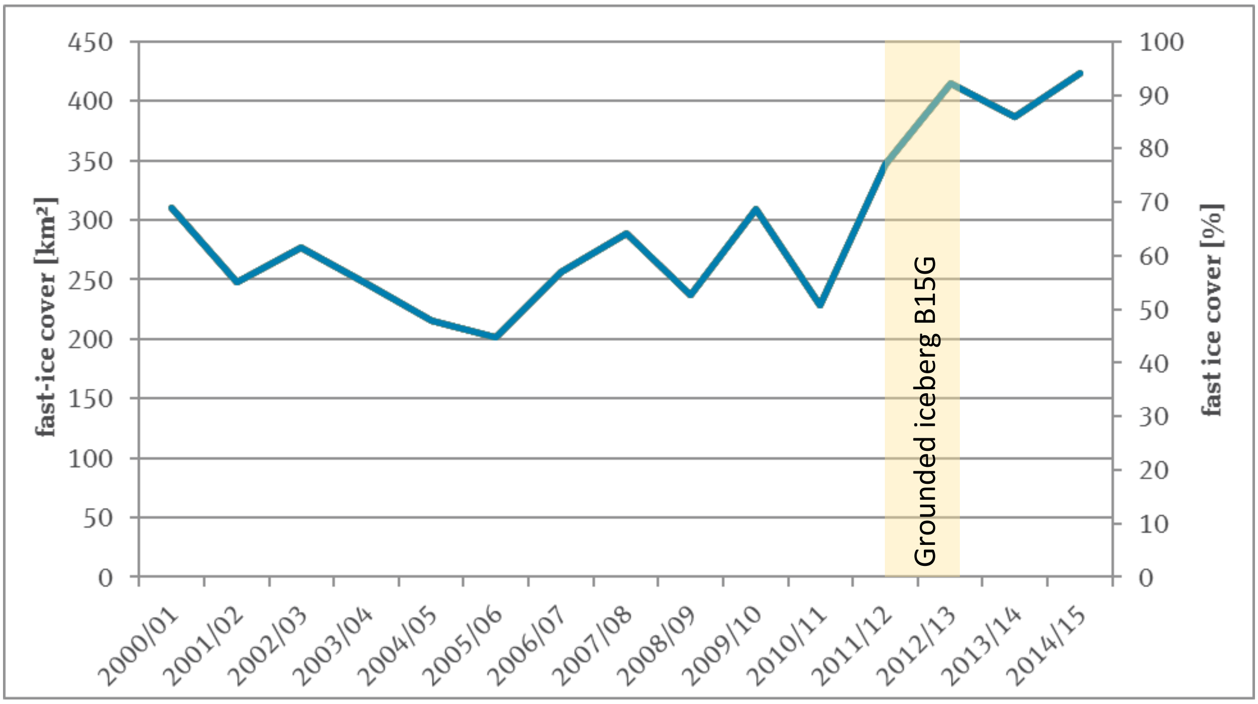

The iceberg dislodged itself in August 2013 and drifted away westward with the coastal current (Hoppmann et al. 2015b, JGR). In September 2010, there was another large iceberg north of Atka Bay, but it did not ground and drifted westward with the coastal current in a few days (Hoppmann et al. 2011). From 2000 to now, there is no indication of more blocking situations by icebergs from the satellite images. The trend of an increasing ice cover is in coincidence with Reid et al (2015) who found a record maximum sea-ice extent in Antarctica for 2013. But this record for the whole sea ice of Antarctica is hardly comparable to the conditions of a single bay as used in this study.

Figure 8: Changes of fast-ice cover of Atka Bay by months

3.2 Spatial distribution

To analyze the spatial distribution of landfast sea ice in Atka Bay an additive overlay of the delineated monthly ice cover was performed. Figure 9 shows the results for the seasons 2000/01 – 2014/15 with dark blue colors symbolizing zones with rare and light colors for zones with frequent ice coverage. The number of months with landfast sea-ice coverage varies considerably from 19 up to 108 of 120 months in total. It is not surprising, that the inner parts of the bay are more often ice covered than the zones that are closer to the open waters of the Southern Ocean. But another feature characterizing the spatial pattern of the ice dynamics is revealed by this data too: The zones with the highest numbers of months with coverage of landfast sea ice are to be found in the southwestern part of Atka Bay.

Figure 9: Total frequency/density of the fast-ice for the seasons 2000/01 - 2014/15 (120 months)

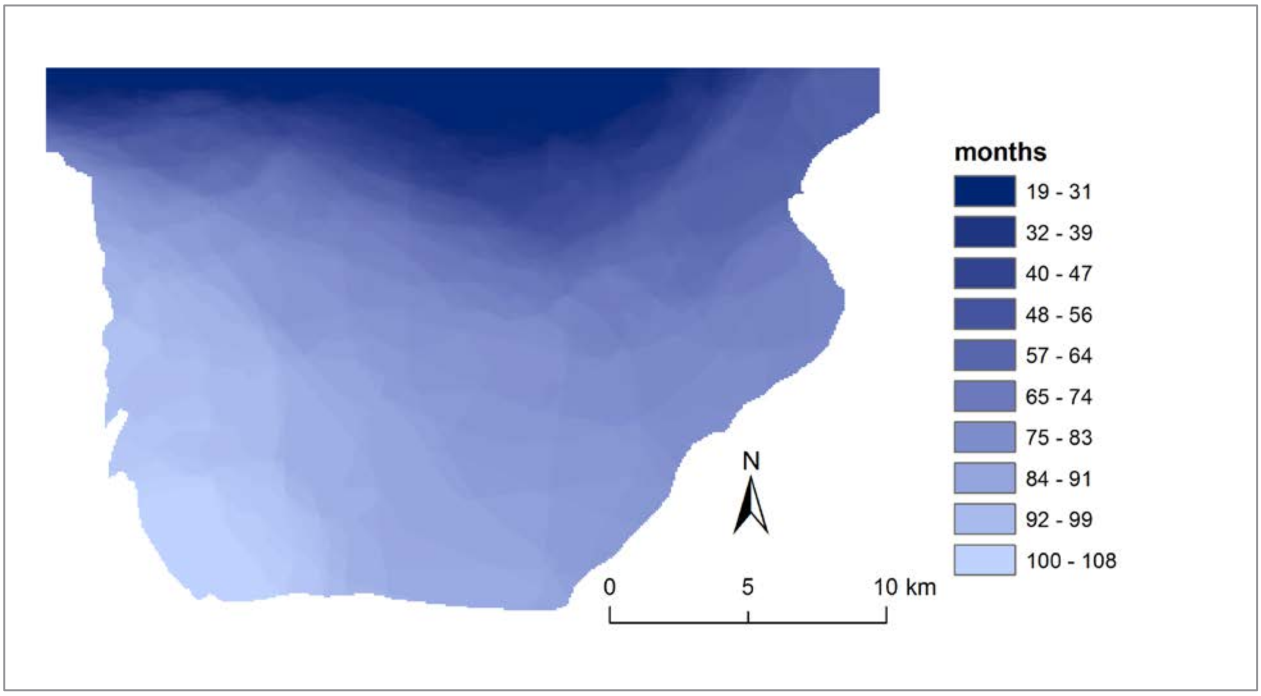

Figure 10 illustrates the spatio-temporal pattern of fast-ice cover distribution differentiated by months. It shows that the ice cover in most seasons is consolidated throughout September, October and November, where it usually has its highest amount of coverage. In this phase there is some variation in the ice cover close to the Southern Ocean where more dynamics of polynyas and leads can be assumed. Later, in December and January, more and more break-ups of the landfast sea ice occur predominantly in the northwestern part. It can clearly be seen, that February and March are the months with the least ice coverage. Likewise it can be seen, that in these months the highest probability of fast-ice occurrence is in the southwestern part of Atka Bay. The pattern for April shows the highest variation of ice coverage, but again a distinct concentration of fast ice in the southwestern part is visible. This leads to the hypothesis, that the building up of sea ice in this part as well benefits from the strong easterlies, which were already mentioned above.

Figure 10: Frequency/Density of the fast-ice cover per month for the seasons 2000/01 - 2014/15 (120 months)

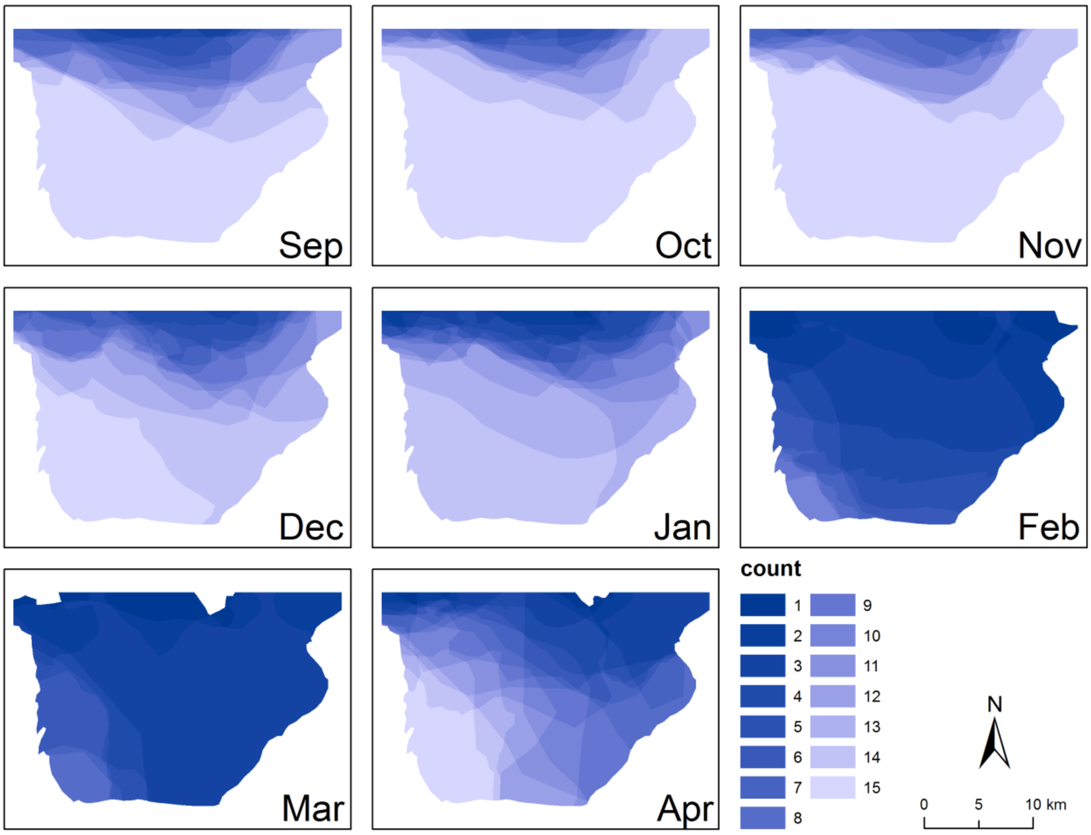

The spatio-temporal patterns over the observation period are displayed in Figure 11. The different extends of the landfast sea ice of all studied years are grouped by months. It can be seen that the reddish colors, displaying the last years, are predominantly arranged close to the northern part in proximity of the open sea. In difference yellow and greenish lines tend to run more in the inner part of Atka Bay. This observation matches with a general increase of fast ice extent during that years presumably triggered by the occurrence of a huge iceberg blocking the entrance of the bay in 2012/13 (see chapter 3.1). Like in this example the data reflect the same temporal dynamic that was already shown in Figure 8 and the spatial variation displayed in Figure 10. Additionally, it can be seen that the general spatial pattern does not change by time. In any case the ice cover of the southwestern part seems to be the most stable, while the northern and northeastern section are the first parts that break up and the last ones that freeze again.

Figure 11: Borders of the fast-ice cover per month for the seasons 2000/01 - 2014/15

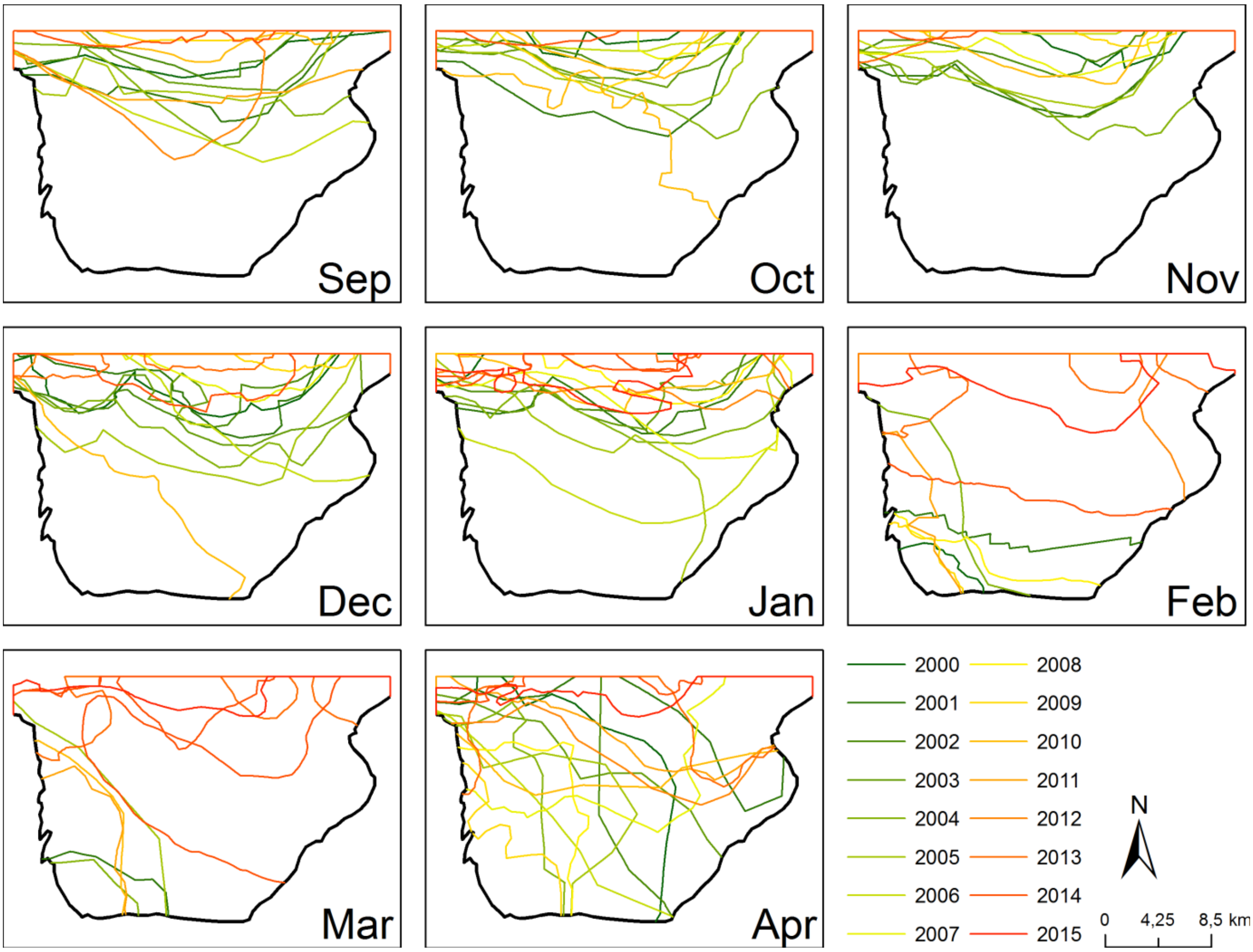

3.3 Penguin breeding site

An emperor penguin colony is located at the south-western part of the Atka Bay (see chapter2.5 & Figure 12). Depending on the quality of the satellite image it was not possible to determine the position of the penguin colony for all time steps. In total the location of the colony could be delineated at 25 images (see Figure 17). Due to the method of delineating the area (see chapter2.5) the sizes for the single years are not comparable. However the comparison of the colony positions revealed a noticeable change to more and more northern positions (Figure 13). In two of the images it was even discovered that the penguins found a way to climb up the Ekström Ice Shelf (Figure 14 & Figure 15). Only one of these occurrences has already been reported before (Zitterbart et al. 2014). Remarkably the climbing up the ice shelf seemed not to be forced by loss or threat of the breeding site on the fast ice, as its ice cover appeared to be intact in both cases. Observations of Zitterbart et al. (2014) indicate that formation of flat snow ramps due to larges snow accumulation allows transition to the ice shelf (Figure 16). However, the majority of the indi-viduals seem to prefer the sheltered lee sides of the embayments that were formed by large cracks in the ice shelf as described by Harris et al. (2015).

Figure 12: Investigation area with the maximum extent of the emperor penguin colony in different years

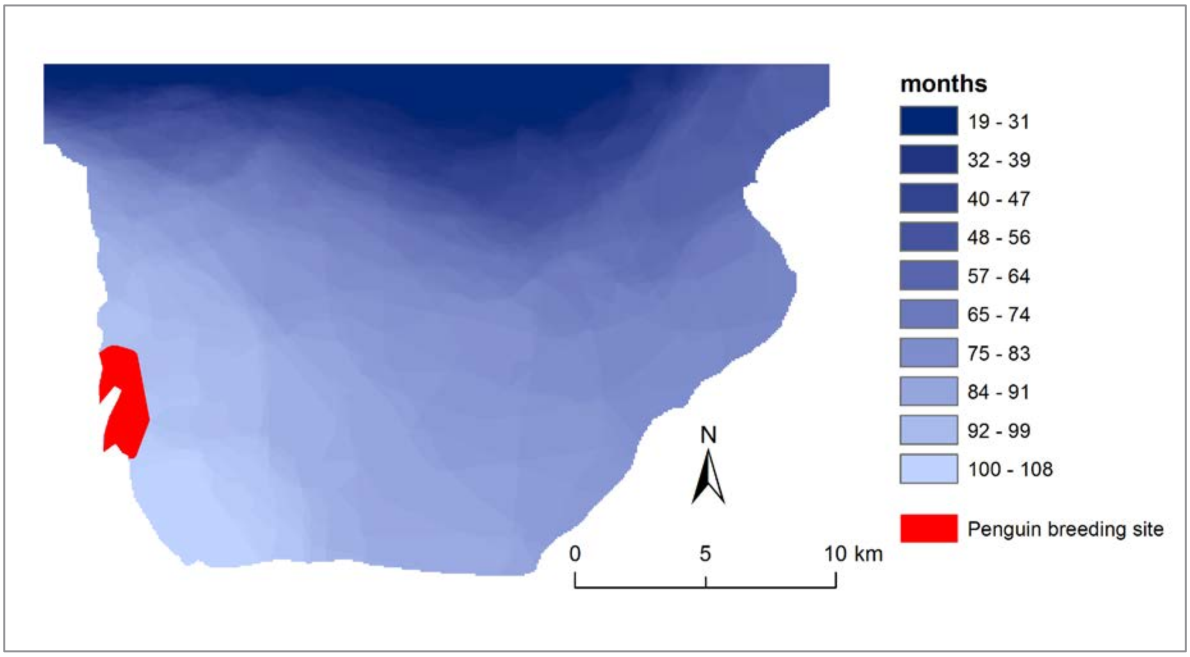

Figure 13: Location/Position of the emperor penguin colony during the investigation period

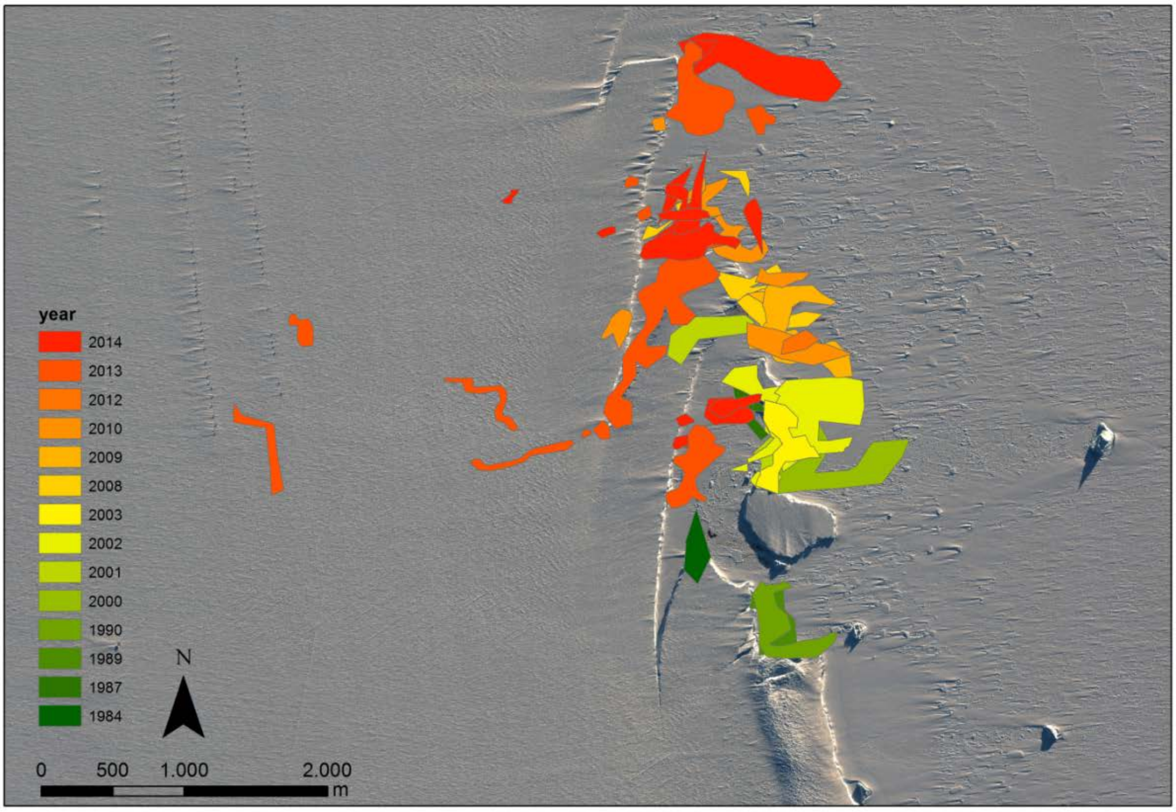

Background image RGB WorldView-2, 50 cm ground resolution, 03 Sep 2012 © Digitalglobe 2012

Figure 14: Probable guano stains and/or emperor penguins at the top of the shelf ice west of the main emperor penguin (RGB; 15 m ground resolution; 7 Dec 2013)

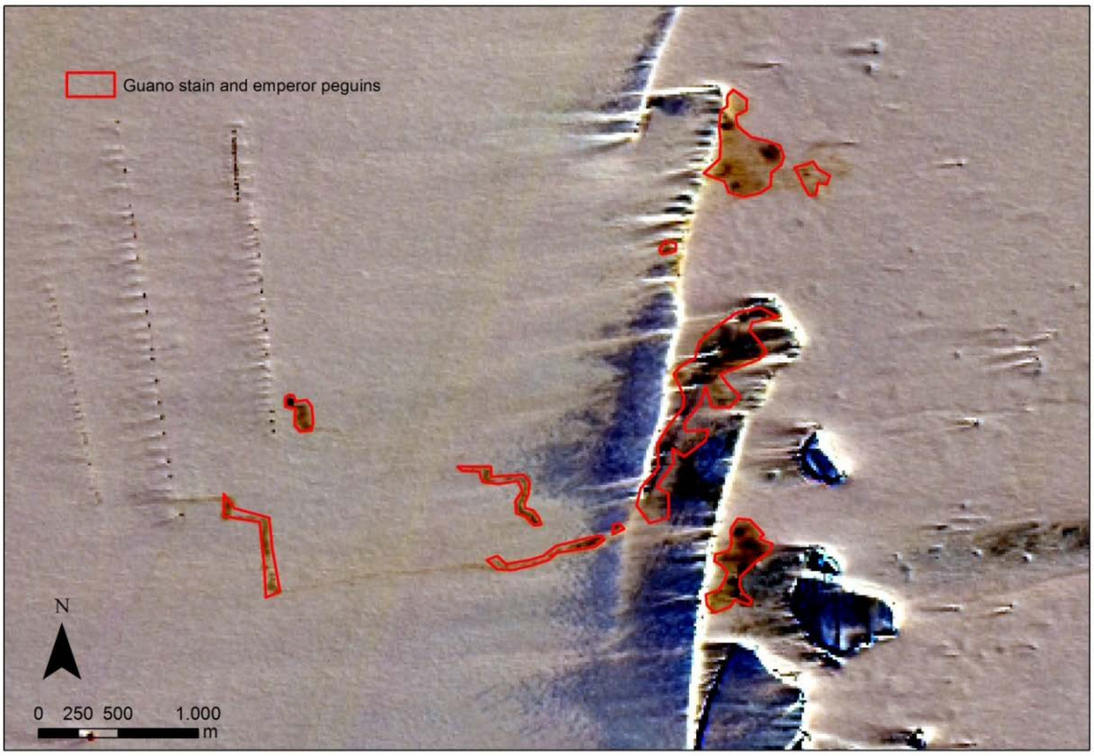

Background image Landsat 8; by courtesy of NASA GSFC & USGS

Figure 15: Probable guano stains at the top of the shelf ice west of the main emperor penguin colony (RGB; 15 m ground resolution; 14 Oct 2014)

Background image Landsat 8; by courtesy of NASA GSFC & USGS

Figure 16: Flat snow ramp allowing the transition from sea ice to shelf ice

© Fritz Hertel 2013

The fast ice of Atka Bay usually breaks up during January/February while it freezes again in March/April. Hence the period in between gives the limits of the penguin breeding season. To examine the stability of these limits the ice-free months at the breeding were analyzed. For this purpose a convex hull was formed by use of all available determined breeding site positions (Figure 13). As the study focuses on fast ice the ice shelf portion was clipped off this area. Comparing the thus defined historic breeding area with the spatial distribution of the ice cover (Figure 9 & Figure 10) it is striking, that obviously the penguins had chosen the area with the highest probability of long lasting solid ground.

Figure 17: Occurrence of landfast sea ice at penguin breeding area

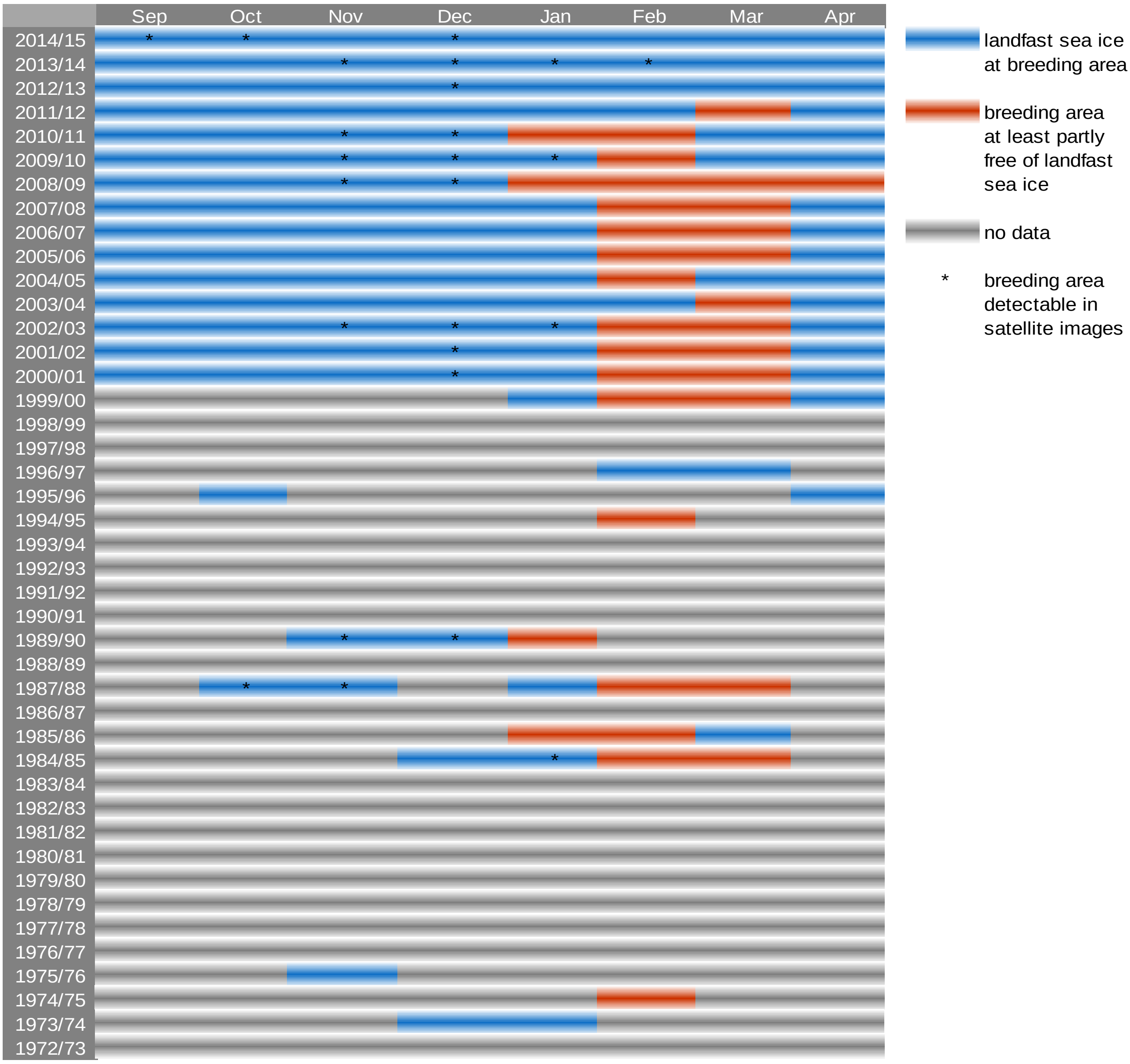

The distribution of ice-free months at the breeding area is displayed in Figure 17. The same data grouped by seasons and grouped by months are shown in Figure 18 and Figure 19. It indicates that the area in most of the studied seasons was free of landfast sea ice in February (10 times) and March (9 times). At two seasons it broke up already in January. Only at one time the ice cover did not form until April. The maximum extend of the ice-free period can reach up to four month (2008/09) while in the most cases it lasts for two months. No clear trend to a more frequent early break-up could be found. Contrariwise, the ice at breeding site was not broken off at all during the last 3 seasons. The timing of the ice formation did not show any trend as well.

Figure 18: Number of seasons without ice cover at the emperor penguin breeding site of Atka Bay per month (seasons 2000/01-2014/15)

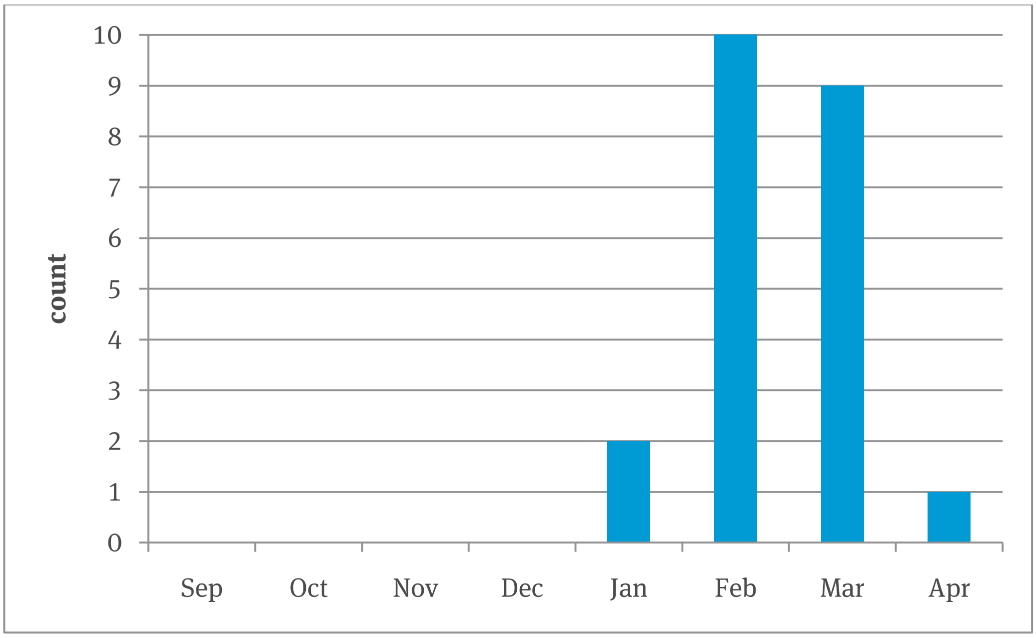

Figure 19: Months per season without cover at the emperor penguin breeding site of Atka Bay (2000/01-2014/15)

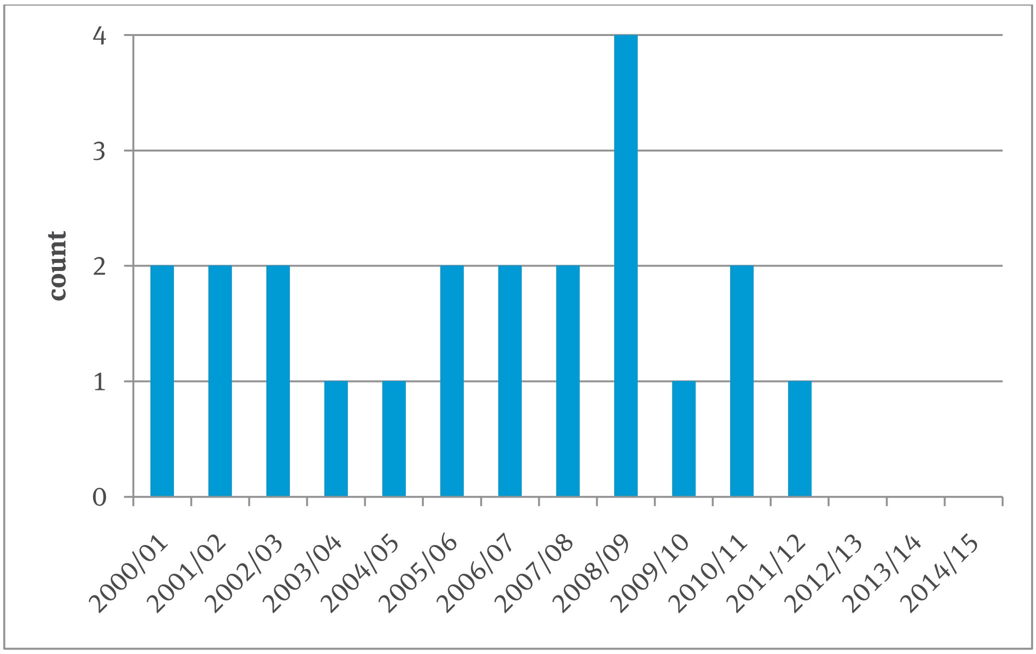

4 Discussion

The temporal evolution of the landfast sea-ice cover in Atka Bay of the seasonal period considered in this study (September to April) reveals no significant trend from 2000/2001 to the austral summer 2010/2011. In this period, the mean values of ice coverage vary between 44 and 68% (201 and 310 km²) (see Figure 7). Starting with the season of 2011/2012, the mean landfast sea-ice coverage of Atka Bay is distinctive higher than in the previous years (75 %; 347 km²). The ice dynamics of the next season (2012/2013) is characterized by the presence of a large grounded iceberg in the northern part of Atka Bay, which might have prevented the break-up of the sea ice. As described in chapter 3.1, in the next season of 2013/2014, when the iceberg has drifted away, the sea ice became thicker second-year ice that probably hampered the break-up of the landfast sea ice again (Hoppmann, 2015a). But in the last season considered in this study (2014/2015), again the landfast sea ice of Atka Bay did not break up completely. Because of the short time of significant higher mean ice coverage it is not possible to figure out the reason for this signal. In the season before the blocking event a higher mean value of landfast sea-ice cover was recorded. This and the fact that the ice did not break up completely in 2014/2015 could be an indication, that other processes than only the blocking are involved. It remains unclear whether the observed signal of mean landfast sea-ice cover in Atka bay is just the result of the blocking by an iceberg or the beginning of a long term trend of increasing ice cover as it was found by Reid et al. (2015) for the sea ice around the Antarctic continent.

Global climate model simulations fail to predict Antarctic sea ice evolution correctly since they predict a distinct loss of sea ice in the 21st century (Sen Gupta et al. 2009) in contrast to the field observations (e.g. Reid et al. 2015). This mismatch is an indication that key processes are missing in the implementation of the models (Turner et al. 2013). It obviously lacks a deeper understanding of the processes that force sea ice dynamics. One important piece of the puzzle might be the interactions and feedback processes between the sea-ice cover and the Antarctic ice shelves (Bintanja et al. 2013, Hoppmann 2015a). As described in chapter 1.2, the accumulation of platelet ice underneath the sea ice is one aspect of these shelf ice/sea ice interactions. According to Hoppmann et al (2015a) 20% of the basal melt volume of Ekström Ice Shelf is refrozen as ice platelets trapped under Atka Bay landfast sea ice. The accumulation and incorporation of platelets leads to an overall contribution to first-year sea ice mass of about 50% in Atka Bay.

The most remarkable feature of the spatio-temporal dynamics of the landfast sea-ice cover of Atka Bay is the occurrence of a relatively robust zone in the southwestern part of the bay. In this area the ice breaks up later in the season and forms again earlier than in other parts (Figure 9 & Figure 10). The cause for this stability should be supposed in the greater ice-thickness compared to other zones. Hoppman et al. (2015a) already found this skewed distribution of ice-thickness by measurements along an east-west profile in the central part of Atka Bay. He considered two processes as main causes. First, predominant strong easterly winds that push the ice towards the ice shelf edge in the west. Second, sea water enters Atka Bay from northeast and cools during its westward way across the bay. Additionally, localization of the robust zone may be explained by the distance to the open ocean in the north where higher kinetic disturbances by stronger currents, passing icebergs and coastal polynyas occur.

The analyzed period is too short to make a confident prediction on the development of the breeding area of the Atka Bay penguin colony. But considering the development of the landfast sea-ice cover in the period 2000/01 – 2014/15, there are no indications of a shortened breeding-season area by earlier break-up or later freezing. In short term actually a prolongation of the potential breeding season seems possible. Even if the condition of the landfast sea ice gets worse for the emperor penguins, it appears possible, that they are able to change their breeding area to the shelf ice where they already have been recorded on satellite images. Zitterbart et al. 2014 state that it is not yet clear if changing climate will facilitate the way up the ice shelf by building up more flat snow ramps. Irrespective of that, it seems likely that the center of the colony will remain at landfast sea ice close to the edge of the ice shelf where topography gives more shelter.

5 References

Ancel, A.; Cristofari, R.; Fretwell, P. T.; Trathan, P. N.; Wienecke, B.; Boureau, M.; Morinay, J.; Blanc, S.; Le Maho, Y.; Le Bohec, C. (2014): Emperors in hiding: when ice-breakers and satellites complement each other in Antarctic exploration. In *PloS one* 9 (6), pp. e100404. DOI: 10.1371/journal.pone.0100404.

Arzel, O.; Fichefet, T.; Goosse, H. (2006): Sea ice evolution over the 20th and 21st centuries as simulated by current AOGCMs. In *Ocean Modelling* 12 (3-4), pp. 401–415. DOI: 10.1016/j.ocemod.2005.08.002.

Attema, E.; Desnos, Y.-L.; Duchossois, G. (2000): Synthetic aperture radar in Europe: ERS, Envisat, and beyond. In *Johns Hopkins APL technical digest* 21 (1), pp. 155–161.

Bintanja, R.; van Oldenborgh, G. J.; Drijfhout, S. S.; Wouters, B.; Katsman, C. A. (2013): Important role for ocean warming and increased ice-shelf melt in Antarctic sea-ice expansion. In *Nature Geosci* 6 (5), pp. 376–379. DOI: 10.1038/ngeo1767.

Comiso, J. C.; Nishio, F. (2008): Trends in the sea ice cover using enhanced and compatible AMSR-E, SSM/I, and SMMR data. In *J. Geophys. Res.* 113 (C2). DOI: 10.1029/2007JC004257.

Flato, G. M. (2004): Sea-ice and its response to CO2 forcing as simulated by global climate models. In *Climate Dynamics* 23 (3-4). DOI: 10.1007/s00382-004-0436-7.

Fraser, A. D.; Massom, R. A.; Michael, K. J.; Galton-Fenzi, B. K.; Lieser, J. L. (2012): East Antarctic Landfast Sea Ice Distribution and Variability, 2000–08. In *J. Climate* 25 (4), pp. 1137–1156. DOI: 10.1175/JCLI-D-10-05032.1.

Fretwell, P. T.; Larue, M. A.; Morin, P.; Kooyman, G. L.; Wienecke, B.; Ratcliffe, N.; Fox, A. J.; Fleming, A. H.; Porter, C.; Trathan, P. N. (2012): An emperor penguin population estimate: the first global, synoptic survey of a species from space. In *PLoS ONE* 7 (4), pp. e33751. DOI: 10.1371/journal.pone.0033751.

Fretwell, P. T.; Trathan, P. N. (2009): Penguins from space. Faecal stains reveal the location of emperor penguin colonies. In *Global Ecology and Biogeography* 18 (5), pp. 543–552. DOI: 10.1111/j.1466-8238.2009.00467.x.

Fretwell, P. T.; Trathan, P. N.; Wienecke, B.; Kooyman, G. L. (2014): Emperor Penguins breeding on iceshelves. In *PloS one* 9 (1). DOI: 10.1371/journal.pone.0085285.

Harris, C. M.; Lorenz, K.; Fishpool, L.; Lascelles, B.; Cooper, J.; Coria, N. R.; Croxall, J. P.; Emmerson, L. M.; Fijn, R. C.; Fraser, W. L.; Jouventin, P.; LaRue, M. A.; Le Maho, Y.; Lynch, H. J.; Naveen, R.; Patterson-Fraser, D. L.; Peter, H.-U.; Poncet, S.; Phillips, R. A.; Southwell, C. J.; van Franeker, J. A.; Weimerskirch, H.; Wienecke, B.; Woehler, E. J. (2015): Important Bird Areas in Antarctica 2015. BirdLife International and Environmental Research & Assessment Ltd. Cambridge.

Heinemann, G.; Ebner, L.; Haid, V.; Timmermann, R. (2013): Katabatic winds and polynya dynamics in the Weddell Sea region (Antarctica). EGU General Assembly April 2013, Vienna, Austria, Geophysical Research Abstracts Vol. 15, EGU2013-10191.

Hempel, G. & Stonehouse, R. J. (1987): The winter expedition of research vessel 'Polarstern' to the Antarctic (ANT 5,1–3). Aerial counts of penguins seals and whales in the eastern Weddell Sea. Berichte zur Polarforschung, 39, 227–230.

Hoppmann, M.; Nicolaus, M.; Hunkeler, P. A.; Heil, P.; Behrens, L.-K.; König-Langlo, G.; Gerdes, R. (2015a): Seasonal evolution of an ice-shelf influenced fast-ice regime, derived from an autonomous thermistor chain. In *J. Geophys. Res. Oceans* 120 (3), pp. 1703–1724. DOI: 10.1002/2014JC010327.

Hoppmann, M.; Nicolaus, M.; Paul, S.; Hunkeler, P. A.; Heinemann, G.; Willmes, S.; Timmermann, R.; Boebel, O.; Schmidt, T.; Kühnel, M.; König-Langlo, G.; Gerdes, R. (2015b): Ice platelets below Weddell Sea landfast sea ice. In *Annals of Glaciology* 56 (69), pp. 175–190. DOI: 10.3189/2015AoG69A678.

Hoppmann, M.; Nicolaus, M.; Schmithüsen, H. (2011): Summary of AFIN measurements on Atka Bay landfast ice in 2010. Alfred Wegener Institute for Polar and Marine Research. Bremerhaven. Available online at https://epic.awi.de/24642/1/Hop2011d.pdf, checked on 11/25/2015.

Hoppmann, M.; Paul, S.; Hunkeler, P.; Baltes, U.; Kühnel, M.; Schmidt, T.; Nicolaus, M.; Heinemann, G.; Willmes, S. (2013): Field work on Atka Bay landfast sea ice in 2012/13. Alfred-Wegener-Institut.

Japan Aerospace Exploration Agency (2015): Alos User Handbook. Available online at http://www.eorc.jaxa.jp/ALOS/en/doc/alos_userhb_en.pdf, checked on 11/25/2015.

Jenouvrier, S.; Caswell, H.; Barbraud, C.; Holland, M.; Stroeve, J.; Weimerskirch, H. (2009): Demographic models and IPCC climate projections predict the decline of an emperor penguin population. In *Proceedings of the National Academy of Sciences* 106 (27), p. 11425. DOI: 10.1073/pnas.0905666106.

Jenouvrier, S.; Holland, M.; Stroeve, J.; Serreze, M.; Barbraud, C.; Weimerskirch, H.; Caswell, H. (2014): Projected continent-wide declines of the emperor penguin under climate change. In *Nature Climate change* 4 (8), pp. 715–718. DOI: 10.1038/nclimate2280.

Jouventin, P.; Barbraud, C.; Rubin, M. (1995): Adoption in the emperor penguin, Aptenodytes forsteri. In *Animal Behaviour* 50 (4), pp. 1023–1029.

Kim, M.; Im, J.; Han, H.; Kim, J.; Lee, S.; Shin, M.; Kim, H.-C. (2015): Landfast sea ice monitoring using multisensor fusion in the Antarctic. In *GIScience & Remote Sensing* 52 (2), pp. 239–256. DOI: 10.1080/15481603.2015.1026050.

Klöwer, M.; Jung, T.; König-Langlo, G.; Semmler, T. (2013): Aspects of weather parameters at Neumayer station, Antarctica, and their representation in reanalysis and climate model data. In *Meteorol. Z.* 22 (6), pp. 699–709. DOI: 10.1127/0941-2948/2013/0505.

König-Langlo, G.; King, J. C.; Pettré, P. (1998): Climatology of the three coastal Antarctic stations Dumont d'Urville, Neumayer, and Halley. In *Journal of Geophysical Research* 103 (D9), pp. 10935–10946.

König-Langlo, G.; Loose, B. (2007): The Meteorological Observatory at Neumayer Stations (GvN and NM-II) Antarctica. In *Polarforschung* 76 (1-2), pp. 25–38.

Langhorne, P. J.; Hughes, K. G.; Gough, A. J.; Smith, I. J.; Williams, M. J. M.; Robinson, N. J.; Stevens, C. L.; Rack, W.; Price, D.; Leonard, G. H.; Mahoney, A. R.; Haas, C.; Haskell, T. G. (2015): Observed platelet ice distributions in Antarctic sea ice. An index for ocean-ice shelf heat flux. In *Geophys. Res. Lett.* 42 (13), pp. 5442–5451. DOI: 10.1002/2015GL064508.

Liu, J. (2004): Interpretation of recent Antarctic sea ice variability. In *Geophys. Res. Lett.* 31 (2). DOI: 10.1029/2003GL018732.

Massom, R. A.; Hill, K.; Barbraud, C.; Adams, N.; Ancel, A.; Emmerson, L.; Pook, M. J. (2009): Fast ice distribution in Adélie Land, East Antarctica. Interannual variability and implications for emperor penguins Aptenodytes forsteri. In *Mar. Ecol. Prog. Ser.* 374, pp. 243–257. DOI: 10.3354/meps07734.

NASA, National Aeronautics and Space Administration (2011): Landsat 7 Science Data Users Handbook. National Aeronautics and Space Administration. Available online at http://landsathandbook.gsfc.nasa.gov/pdfs/Landsat7_Handbook.pdf.

Nihashi, S.; Ohshima, K. I. (2015): Circumpolar Mapping of Antarctic Coastal Polynyas and Landfast Sea Ice. Relationship and Variability. In *J. Climate* 28 (9), pp. 3650–3670. DOI: 10.1175/JCLI-D-14-00369.1.

Parkinson, C. L.; Cavalieri, D. J. (2012): Antarctic sea ice variability and trends, 1979-2010. In *The Cryosphere* 6 (4), pp. 871–880. DOI: 10.5194/tc-6-871-2012.

Pfeifer, C.; Hertel, F.; Kopp, M.; Metzig, R.; Mustafa, O.; Peter, H.-U.; Weimerskirch, H. (2013): Satellite based monitoring of emperor penguin colonies in the Antarctic. In SCAR (Ed.): Life in Antarctica: Boundaries and Gradients in a Changing Environment. Book of Abstracts. XIth SCAR Biology Symposium. Barcelona, July, 15-19.

Reid, P.; Stammerjohn, S.; Massom, R.; Scambos, T.; Lieser, J. (2015): The record 2013 Southern Hemisphere sea-ice extent maximum. In *Annals of Glaciology* 56 (69), pp. 99–106. DOI: 10.3189/2015AoG69A892.

Schneider, D. P.; Deser, C.; Okumura, Y. (2012): An assessment and interpretation of the observed warming of West Antarctica in the austral spring. In *Clim Dyn* 38 (1-2), pp. 323–347. DOI: 10.1007/s00382-010-0985-x.

Schwegmann, S. (2012): Interannual and decadal variability of sea ice drift, concentration and thickness in the Weddell Sea.

Sen Gupta, A.; Santoso, A.; Taschetto, A. S.; Ummenhofer, C. C.; Trevena, J.; England, M. H. (2009): Projected Changes to the Southern Hemisphere Ocean and Sea Ice in the IPCC AR4 Climate Models. In *J. Climate* 22 (11), pp. 3047–3078. DOI: 10.1175/2008JCLI2827.1.

Teschke, K.; Beaver, D.; Bester, M.; Bombosch, A.; Bornemann, H.; Brandt, A.; Brtnik, P.; Broyer, C. de; Burkhardt, E.; Dieckmann, G.; Douglas, L.; Flores, H.; Gerdes, D.; Griffiths, H.; Gutt, J.; Hain, S.; Hauck, J.; Hellmer, H.; Herata, H.; Hoppema, M.; Isla, E.; Jerosch, K.; Kock, K.-H.; Krause, R.; Kuhn, G.; Lemke, P.; Liebschner, A.; Linse, K.; Miller, H.; Mintenbeck, K.; Nixdorf, U.; Pehlke, H.; Petrov, A.; Schröder, M.; Shust, K.; Schwegmann, S.; Siegel, V.; Thomisch, K.; Timmermann, R.; Trathan, P. N.; van de Putte, A.; van Frakener, J. A.; van Opzeeland, I.; Nordheim, H. von; Brey, T.: Scientific background document in support of the development of CCAMLR MPA in the Weddell Sea (Antarctica) – Version 2015 information on Weddell Sea MPA planning area. Part A: General context of the establishment of MPAs and background. CCAMLR.

Turner, J.; Bracegirdle, T. J.; Phillips, T.; Marshall, G. J.; Hosking, J. S. (2013): An Initial Assessment of Antarctic Sea Ice Extent in the CMIP5 Models. In *J. Climate* 26 (5), pp. 1473–1484. DOI: 10.1175/JCLI-D-12-00068.1.

Turner, J.; Hosking, J. S.; Bracegirdle, T. J.; Marshall, G. J.; Phillips, T. (2015a): Recent changes in Antarctic Sea Ice. In *Philosophical transactions. Series A, Mathematical, physical, and engineering sciences* 373 (2045). DOI: 10.1098/rsta.2014.0163.

Turner, J.; Hosking, J. S.; Marshall, G. J.; Phillips, T.; Bracegirdle, T. J. (2015b): Antarctic sea ice increase consistent with intrinsic variability of the Amundsen Sea Low. In *Clim Dyn. DOI:* 10.1007/s00382-015-2708-9.

USGS (2015): Landsat - A Global Land-Imaging Mission. Available online at http://pubs.usgs.gov/fs/2012/3072/fs2012-3072.pdf, checked on 11/25/2015.

van den Broeke, M.; König-Langlo, G.; Picard, G.; Kuipers Munneke, P.; Lenaerts, J. (2010): Surface energy balance, melt and sublimation at Neumayer Station, East Antarctica. In *Antarctic Science* 22 (01), p. 87. DOI: 10.1017/S0954102009990538.

van Franeker, J. A.; Feij, B.; Flores, H.; Meijboom, A.; van Dorssen, M. (2010): Marine birds and mammals in the Lazarev Sea: The summer influx. In U. Bathmann (Ed.): The expedition of the research vessel "Polarstern" to the Antarctic in 2007/2008 (ANT-XXIV/2). Berichte zur Polar- und Meeresforschung (Reports on Polar and Marine Research). Bremerhaven (604).

Vaughan, D. G.; Marshall, G. J.; Connolley, W. M.; Parkinson, C.; Mulvaney, R.; Hodgson, D. A.; King, J. C.; Pudsey, C. J.; Turner, J. (2003): Recent Rapid Regional Climate Warming on the Antarctic Peninsula. In *Climatic Change* 60 (3), pp. 243–274. Available online at http://www.era.gs/resources/iba/Important_Bird_Areas_in_Antarctica_2015_v5.pdf.

Vermote, E. F.; Kotchenova, S. Y.; Ray, J. P. (2011): MODIS surface reflectance user's guide. MODIS Land Surface Reflectance Science Computing Facility (1). Available online at http://modis-sr.ltdri.org/guide/MOD09_UserGuide_v1_3.pdf, checked on 11/25/2015.

WMO (2014): Sea Ice Nomenclature. (WMO No. 259 volume 1 – Terminology and Codes, Volume II –Illustrated Glossary and III – International System of Sea-Ice Symbols).

Zitterbart, D. P.; Richter, S.; Spiekermann, G.; Behrens, L. K.; Regnery, J.; Fontes, R. P.; Hänssler, T.; König-Langlo, G.; Weller, R.; Fabry, B. (2014): Are environmental factors responsible for changed breeding behaviour in emperor penguins? In *Antarctic Science* 26 (05), pp. 563–564. DOI: 10.1017/S0954102014000285.

Zwally, H. J. (2002): Variability of Antarctic sea ice 1979–1998. In *J. Geophys. Res.* 107 (C5). DOI: 10.1029/2000JC000733.